

Convolutional Hypercomplex Embeddings for Link Prediction

Caglar Demir

Data Science Research Group, Paderborn University

CAGLAR.DEMIR@UPB.DE

Diego Moussallem

*Data Science Research Group, Paderborn University
Globo, Rio de Janeiro, Brazil*

DIEGO.MOUSSALLEM@UPB.DE

Stefan Heindorf

Data Science Research Group, Paderborn University

HEINDORF@UPB.DE

Axel-Cyrille Ngonga Ngomo

Data Science Research Group, Paderborn University

AXEL.NGONGA@UPB.DE

Abstract

Knowledge graph embedding research has mainly focused on the two smallest normed division algebras, \mathbb{R} and \mathbb{C} . Recent results suggest that trilinear products of quaternion-valued embeddings can be a more effective means to tackle link prediction. In addition, models based on convolutions on real-valued embeddings often yield state-of-the-art results for link prediction. In this paper, we investigate a composition of convolution operations with hypercomplex multiplications. We propose the four approaches QMULT, OMULT, CONVQ and CONVO to tackle the link prediction problem. QMULT and OMULT can be considered as quaternion and octonion extensions of previous state-of-the-art approaches, including DistMult and ComplEx. CONVQ and CONVO build upon QMULT and OMULT by including convolution operations in a way inspired by the residual learning framework. We evaluated our approaches on seven link prediction datasets including WN18RR, FB15K-237 and YAGO3-10. Experimental results suggest that the benefits of learning hypercomplex-valued vector representations become more apparent as the size and complexity of the knowledge graph grows. CONVO outperforms state-of-the-art approaches on FB15K-237 in MRR, Hit@1 and Hit@3, while QMULT, OMULT, CONVQ and CONVO outperform state-of-the-art approaches on YAGO3-10 in all metrics. Results also suggest that link prediction performances can be further improved via prediction averaging. To foster reproducible research, we provide an open-source implementation of approaches, including training and evaluation scripts as well as pretrained models.¹

Keywords: Convolution, Hypercomplex Embeddings, Link Prediction, Residual Learning

1. Introduction

Knowledge graphs represent structured collections of facts describing the world in the form of typed relationships between entities (Hogan et al., 2020). These collections of facts have been used in a wide range of applications, including web search, question answering, recommender systems, cancer research, machine translation, and even entertainment (Eder, 2012; Bordes et al., 2014; Zhang et al., 2016; Saleem et al., 2014; Moussallem et al., 2019; Malyshev et al., 2018). However, most knowledge graphs on the web are far from complete (Nickel

1. <https://github.com/dice-group/Convolutional-Hypercomplex-Embeddings-for-Link-Prediction>

et al., 2015). The task of identifying missing links in knowledge graphs is referred to as *link prediction*. Knowledge Graph Embedding (KGE) models have been particularly successful at tackling the link prediction task, among many others (Nickel et al., 2015).

KGE research has mainly focused on the two smallest normed division algebras—real numbers (\mathbb{R}) and complex numbers (\mathbb{C})—neglecting the benefits of the larger normed division algebras—quaternions (\mathbb{H}) and octonions (\mathbb{O}). While Yang et al. (2015) introduced the trilinear product of *real*-valued embeddings $\langle \mathbf{e}_h, \mathbf{e}_r, \mathbf{e}_t \rangle$ of triples $(\mathbf{h}, \mathbf{r}, \mathbf{t})$ as a scoring function for link prediction, Trouillon et al. (2016) showed the usefulness of the Hermitian product of *complex*-valued embeddings $\text{Re}(\langle \mathbf{e}_h, \mathbf{e}_r, \overline{\mathbf{e}_t} \rangle)$: in contrast to *real*-valued embeddings, this product is not symmetric and can be used to model antisymmetric relations since $\text{Re}(\langle \mathbf{e}_t, \mathbf{e}_r, \overline{\mathbf{e}_h} \rangle) \neq \text{Re}(\langle \mathbf{e}_t, \mathbf{e}_r, \overline{\mathbf{e}_h} \rangle)$. To further increase the expressivity, Zhang et al. (2019) proposed learning *quaternion*-valued embeddings due to their benefits over *complex*-valued embeddings. Recently, Zhang et al. (2021) show that replacing a fully-connected layer with a hypercomplex multiplication layer in a neural network leads to significant parameter efficiency without degenerating predictive performance in many tasks including natural language inference, machine translation and text style transfer.

Nguyen et al. (2017); Dettmers et al. (2018); Balažević et al. (2019b); Demir and Ngomo (2021) showed that convolutions are another effective means to increase the expressivity: the sparse connectivity property of the convolution operator endows models with parameter efficiency—unlike models simply increasing the embedding size which is not scalable to large knowledge graphs (Dettmers et al., 2018). Different configurations of the number of feature maps and the shape of kernels in the convolution operation are often explored to find the best ratio between expressiveness and parameter space size.

We investigate the use of convolutions on hypercomplex embeddings by proposing four models: QMULT and OMULT can be considered hypercomplex extensions of DistMult (Yang et al., 2015) in \mathbb{H} and \mathbb{O} , respectively. In contrast to the state of the art (Zhang et al., 2019), we address the scaling effect of multiplication in \mathbb{H} and \mathbb{O} by applying the batch normalization technique. Through the batch normalization technique, QMULT and OMULT are allowed to control the rate of normalization and benefit from its implicit regularization effect (Ioffe and Szegedy, 2015). Importantly, Lu and Hu (2020) suggest that using solely unit quaternion-based rotations between head entity and relation limits the modeling capacity for various types of relations. CONVQ and CONVO build upon QMULT and OMULT by including the convolution operator in a way inspired by the residual learning framework (He et al., 2016). CONVQ and CONVO forge QMULT and OMULT with a 2D convolution operation and an affine transformation via the Hadamard product, respectively. By virtue of this architecture, we show that CONVQ can degenerate QMULT, ComplEx or DistMult, if such degeneration is necessary to further minimize the training loss (see Equations (6) and (10)).

Experiments suggest that our models often achieve state-of-the-art performance on seven benchmark datasets (WN18, FB15K, WN18RR, FB15K-237, YAGO3-10, Kinship and UMLS). Superiority of our models against state-of-the-art models increases as the size and complexity of the knowledge graph grows. Our results also indicate that generalization performances of models can be further increased by applying ensemble learning.

2. Related Work

In the last decade, a plethora of KGE approaches have been successfully applied to tackle various tasks (Nickel et al., 2015; Cai et al., 2018; Ji et al., 2020). In this section, we give a brief chronological overview of selected KGE approaches. RESCAL computes a three-way factorization of a third-order adjacency tensor representing the input knowledge graph to compute scores for triples (Nickel et al., 2011). RESCAL captures various types of relations in the input KG but is limited in its scalability as it has quadratic complexity in the factorization rank (Trouillon et al., 2017). DistMult can be regarded as an efficient extension of RESCAL with a diagonal matrix per relation to reduce the complexity of RESCAL (Yang et al., 2015). DistMult performs poorly on antisymmetric relations, whereas performing well on symmetric relations (Trouillon et al., 2016). ComplEx extends DistMult by learning representations in a complex vector space (Trouillon et al., 2016). ComplEx is able to infer both symmetric and antisymmetric relations via a Hermitian inner product of embeddings that involves the conjugate-transpose of one of the two input vectors. Lacroix et al. (2018) design two novel regularizers along with a data augmentation technique and propose ComplEx-N3 that can be seen as ComplEx with the N3 regularization. ConvE applies a 2D convolution operation to model the interactions between entities and relations (Dettmers et al., 2018). ConvKB extends ConvE by omitting reshaping operation in the encoding of representations in the convolution operation (Nguyen et al., 2017). Similarly, HypER extends ConvE by applying relation-specific convolution filters as opposed to applying filters from concatenated subject and relation vectors (Balažević et al., 2019b). TuckER employs the Tucker decomposition on the binary tensor representing the input knowledge graph triples (Balažević et al., 2019c). RotatE employs a rotational model taking predicates as rotations from subjects to objects in complex space via the element-wise Hadamard product (Sun et al., 2019). By these means, RotatE performs well on composition relations where other approaches perform poorly. QuatE applies the quaternion multiplication followed by an inner product to compute scores of triples (Zhang et al., 2019).

3. Link Prediction & Hypercomplex Numbers

Link Prediction. Let \mathcal{E} and \mathcal{R} represent the sets of entities and relations. Then, a Knowledge Graph (KG) can be formalised as a set of triples $\mathcal{G} = \{(\mathbf{h}, \mathbf{r}, \mathbf{t})\} \subseteq \mathcal{E} \times \mathcal{R} \times \mathcal{E}$ where each triple contains two entities $\mathbf{h}, \mathbf{t} \in \mathcal{E}$ and a relation $\mathbf{r} \in \mathcal{R}$. The link prediction problem is formalised by learning a scoring function $\phi : \mathcal{E} \times \mathcal{R} \times \mathcal{E} \mapsto \mathbb{R}$ ideally characterized by $\phi(\mathbf{h}, \mathbf{r}, \mathbf{t}) > \phi(\mathbf{x}, \mathbf{y}, \mathbf{z})$ if $(\mathbf{h}, \mathbf{r}, \mathbf{t})$ is true and $(\mathbf{x}, \mathbf{y}, \mathbf{z})$ is not (Dettmers et al., 2018).

Hypercomplex Numbers. The quaternions are a 4-dimensional normed division algebra (Hamilton, 1844; Baez, 2002). A quaternion number $Q \in \mathbb{H}$ is defined as $Q = a + b\mathbf{i} + c\mathbf{j} + d\mathbf{k}$ where a, b, c, d are real numbers and $\mathbf{i}, \mathbf{j}, \mathbf{k}$ are imaginary units satisfying Hamilton’s rule: $\mathbf{i}^2 = \mathbf{j}^2 = \mathbf{k}^2 = \mathbf{ijk} = -1$. Let Q_1 and $Q_2 \in \mathbb{H}$ be two quaternions, the inner product $Q_1 \cdot Q_2 \in \mathbb{R}$ of two quaternions is defined as

$$Q_1 \cdot Q_2 = a_1a_2 + b_1b_2 + c_1c_2 + d_1d_2.$$

The quaternion multiplication of Q_1 and Q_2 is defined as

$$\begin{aligned} Q_1 \otimes Q_2 &= (a_1a_2 - b_1b_2 - c_1c_2 - d_1d_2) \\ &\quad + (a_1b_2 + b_1a_2 + c_1d_2 - d_1c_2) \mathbf{i} \\ &\quad + (a_1c_2 - b_1d_2 + c_1a_2 + d_1b_2) \mathbf{j} \\ &\quad + (a_1d_2 + b_1c_2 - c_1b_2 + d_1a_2) \mathbf{k}. \end{aligned}$$

The quaternion multiplication is also known as the Hamilton product (Zhang et al., 2021). For a d -dimensional quaternion vector $a + b \mathbf{i} + c \mathbf{j} + d \mathbf{k}$ with $a, b, c, d \in \mathbb{R}^d$, the inner product and multiplication is defined accordingly. The Octonions are an 8-dimensional algebra where an octonion number $O_1 \in \mathbb{O}$ is defined as $O_1 = x_0 + x_1\mathbf{e}_1 + x_2\mathbf{e}_2 + \dots + x_7\mathbf{e}_7$, where $\mathbf{e}_1, \mathbf{e}_2 \dots \mathbf{e}_7$ are imaginary units (Baez, 2002). Their product (\star), inner product (\cdot) and vector operations are defined analogously to quaternions.

The quaternion multiplication subsumes real-valued multiplication and enjoys a parameter saving with 1/4 as compared to the real-valued matrix multiplication (Parcollet et al., 2018, 2019; Zhang et al., 2021). Leveraging such properties of quaternions in neural networks showed promising results in numerous tasks (Zhang et al., 2021, 2019; Chen et al., 2020). In turn, the octonion multiplication in neural networks and learning octonion-valued knowledge graph embeddings had not been yet fully explored.

4. Convolutional Hypercomplex Embeddings

Motivation. Dettmers et al. (2018) suggest that indegree and PageRank can be used to quantify the difficulty of predicting missing links in KGs. Results indicate that the superiority of ConvE becomes more apparent against DistMult and ComplEx as the complexity of the knowledge graph increases, i.e., indegree and PageRank of a KG increase (see Table 6 in Dettmers et al. (2018)). In turn, Zhang et al. (2019) show that learning quaternion-valued embeddings via multiplicative interactions can be a more effective means of predicting missing links than learning real and complex-valued embeddings. Although learning quaternion-valued embeddings through multiplicative interactions yields promising results, the only way to further increase the expressiveness of such models is to increase the number of dimensions of embeddings. This does not scale to larger knowledge graphs (Dettmers et al., 2018). Increasing parameter efficiency while retaining effectiveness is a desired property in many applications (Zhang et al., 2021; Trouillon et al., 2016, 2017).

Motivated by findings of aforementioned works, we investigate the composition of convolution operations with hypercomplex multiplications. The rationale behind this composition is to increase the expressiveness without increasing the number of parameters. This nontrivial endeavor is the keystone of embedding models (Trouillon et al., 2016). The sparse connectivity property of the convolution operation endows models with parameter efficiency which helps to scale to larger knowledge graphs. Additionally, different configurations of the number of kernels and their shapes can be explored to find the best ratio between expressiveness and the number of parameters. Although increasing the number of feature maps results in increasing the number of parameters, we are able to benefit from the parameter sharing property of convolutions (Goodfellow et al., 2016).

Approaches. Inspired by the early works DistMult and ConvE, we dub our approaches QMULT, OMULT, CONVQ, and CONVO where “Q” represents the quaternion variant and “O” the octonion variant. Given a triple $(\mathbf{h}, \mathbf{r}, \mathbf{t})$, QMULT : $\mathbb{H} \mapsto \mathbb{R}$ computes a triple score through the quaternion multiplication of head entity embeddings \mathbf{e}_h and relation embeddings \mathbf{e}_r followed by the inner product with tail entity embeddings \mathbf{e}_t as

$$\text{QMULT}(h, r, t) = \mathbf{e}_h \otimes \mathbf{e}_r \cdot \mathbf{e}_t, \quad (1)$$

where $\mathbf{e}_h, \mathbf{e}_r, \mathbf{e}_t \in \mathbb{H}^d$. Similarly, OMULT : $\mathbb{O} \mapsto \mathbb{R}$ performs the octonion multiplication followed by the inner product as

$$\text{OMULT}(h, r, t) = \mathbf{e}_h \star \mathbf{e}_r \cdot \mathbf{e}_t, \quad (2)$$

where $\mathbf{e}_h, \mathbf{e}_r, \mathbf{e}_t \in \mathbb{O}^d$. Computing scores of triples in this setting can be illustrated in two consecutive steps: (1) rotating \mathbf{e}_h through \mathbf{e}_r by applying quaternion/octonion multiplication and (2) squishing $(\mathbf{e}_h \otimes \mathbf{e}_r)$ and \mathbf{e}_t into a real number line by taking the inner product. During training, the degree between $(\mathbf{e}_h \otimes \mathbf{e}_r)$ and \mathbf{e}_t is minimized provided $(\mathbf{h}, \mathbf{r}, \mathbf{t}) \in \mathcal{G}$.

Motivated by the response of John T. Graves to W. R. Hamilton,² we combine convolution operations with QMULT and OMULT as defined

$$\text{CONVQ}(h, r, t) = \text{conv}(\mathbf{e}_h, \mathbf{e}_r) \circ (\mathbf{e}_h \otimes \mathbf{e}_r) \cdot \mathbf{e}_t, \quad (3)$$

$$\text{CONVO}(h, r, t) = \text{conv}(\mathbf{e}_h, \mathbf{e}_r) \circ (\mathbf{e}_h \star \mathbf{e}_r) \cdot \mathbf{e}_t, \quad (4)$$

where $\text{conv}(\cdot, \cdot) : \mathbb{H}^{2d} \mapsto \mathbb{R}^{4d}$ (respectively $:\mathbb{O}^{2d} \mapsto \mathbb{R}^{8d}$) is defined as

$$\text{conv}(\mathbf{e}_h, \mathbf{e}_r) = f(\text{vec}(f([\mathbf{e}_h, \mathbf{e}_r] * \omega))) \cdot \mathbf{W} + \mathbf{b}). \quad (5)$$

$f(\cdot)$, $\text{vec}(\cdot)$, $*$, ω , and (\mathbf{W}, \mathbf{b}) denote the rectified linear unit function, a flattening operation, convolution operation, kernel in the convolution and an affine transformation, respectively.

Connection to Complex and DistMult. During training, $\text{conv}(\cdot, \cdot)$ can reduce its range into $\gamma \in 1^{4d}$ if such reduction is necessary to further decrease the training loss. In the following Equations (6) to (10), we elucidate the reduction of CONVQ into QMULT and ComplEx:

$$\text{CONVQ}(\mathbf{h}, \mathbf{r}, \mathbf{t}) = \gamma \circ (\mathbf{e}_h \otimes \mathbf{e}_r) \cdot \mathbf{e}_t. \quad (6)$$

Equation (6) corresponds to QMULT provided that $\text{conv}(\mathbf{e}_h, \mathbf{e}_r) = \gamma = 1^{4d}$. CONVQ can be further reduced into ComplEx by setting the imaginary parts \mathbf{j} and \mathbf{k} of \mathbf{e}_h , \mathbf{e}_r and \mathbf{e}_t to zero:

$$\gamma \circ ((a_h + b_h \mathbf{i}) \otimes (a_r + b_r \mathbf{i})) \cdot (a_t + b_t \mathbf{i}). \quad (7)$$

Computing the quaternion multiplication of two quaternion-valued vectors corresponds to Equation (8):

$$\gamma \circ [(a_h \circ a_r - b_h \circ b_r) + (a_h \circ b_r + b_h \circ a_r) \mathbf{i}] \cdot (a_t + b_t \mathbf{i}). \quad (8)$$

The resulting quaternion-valued vector is scaled with $\gamma = [\gamma_1, \gamma_2]$:

$$[(\gamma_1 \circ a_h \circ a_r - \gamma_1 \circ b_h \circ b_r) + (\gamma_2 \circ a_h \circ b_r + \gamma_2 \circ b_h \circ a_r) \mathbf{i}] \cdot (a_t + b_t \mathbf{i}). \quad (9)$$

2. “If with your alchemy you can make three pounds of gold, why should you stop there?” Baez (2002).

Through taking the inner product of the former vector with $(a_t + b_t \mathbf{i})$, we obtain

$$\begin{aligned} \text{CONVQ}(\mathbf{h}, \mathbf{r}, \mathbf{t}) &= \langle \gamma_1, a_h, a_r, a_t \rangle \\ &\quad + \langle \gamma_2, b_h, a_r, b_t \rangle \\ &\quad + \langle \gamma_2, a_h, b_r, b_t \rangle \\ &\quad - \langle \gamma_1, b_h, b_r, a_t \rangle, \end{aligned} \tag{10}$$

where $\langle a, b, c, d \rangle = \sum_k a_k b_k c_k d_k$ corresponds to the multi-linear inner product. Equation (10) corresponds to ComplEx provided that $\gamma = 1^{4d}$. In the same way, CONVQ can be reduced into DistMult by setting all imaginary parts $\mathbf{i}, \mathbf{j}, \mathbf{k}$ to zero for e_h, e_r and e_t yielding

$$\text{CONVQ}(\mathbf{h}, \mathbf{r}, \mathbf{t}) = \langle \gamma_1, a_h, a_r, a_t \rangle. \tag{11}$$

Connection to residual learning. The residual learning framework facilitates training of deep neural networks. A simple residual learning block consists of two weight layers denoted by $\mathcal{F}(x)$ and an identity mapping of the input x (see Figure 2 in He et al. (2016)). Increasing the depth of a neural model via stacking residual learning blocks led to significant improvements in many domains. In our setting, $\mathcal{F}(\cdot)$ and x correspond to $\text{conv}(\cdot, \cdot)$ and $[\mathbf{e}_h, \mathbf{e}_r]$, respectively. We replaced the identity mapping of the input with the hypercomplex multiplication. To scale the output, we replaced the elementwise vector addition with the Hadamard product. By virtue of such inclusion, CONVQ and CONVO are endowed with the ability of controlling the impact of $\text{conv}(\cdot, \cdot)$ on predicted scores as shown in Equation (10). Ergo, the gradients of loss (see Equation (12)) w.r.t. head entity and relation embeddings can be propagated in two ways, namely, via $\text{conv}(\mathbf{e}_h, \mathbf{e}_r)$ or hypercomplex multiplication. Moreover, the number of feature maps and the shape of kernels can be used to find the best ratio between expressiveness and the number of parameters. Hence, the expressiveness of models can be adjusted without necessarily increasing the embedding size. Although increasing the number of feature maps results in increasing the number of parameters in the model, we are able to benefit from the parameter sharing property of convolutions.

5. Experimental Setup

5.1. Datasets

We used seven datasets: WN18RR, FB15K-237, YAGO3-10, FB15K, WN18, UMLS and Kinship. An overview of the datasets is provided in Table 1. The latter four datasets are included for the sake of the completeness of our evaluation. Dettmers et al. (2018) suggest that indegree and PageRank can be used to indicate difficulty of performing link prediction on an input KG. In our experiments, we are particularly interested in link prediction results on complex KGs. As commonly done, we augment the datasets by adding reciprocal triples $(\mathbf{t}, \mathbf{r}^{-1}, \mathbf{h})$ (Dettmers et al., 2018; Balazević et al., 2019b,c). For link prediction based on only tail entity ranking experiments (see Table 5), we omit the data augmentation on the test set as similarly done by Bansal et al. (2019).

Table 1: Overview of datasets in terms of entities, relations, average node degree plus/minus standard deviation.

Dataset	$ \mathcal{E} $	$ \mathcal{R} $	Degree	$ \mathcal{G}^{\text{Train}} $	$ \mathcal{G}^{\text{Val.}} $	$ \mathcal{G}^{\text{Test}} $
YAGO3-10	123,182	37	9.6±8.7	1,079,040	5,000	5,000
FB15K	14,951	1,345	32.5±69.5	483,142	50,000	59,071
WN18	40,943	18	3.5±7.7	141,442	5,000	5,000
FB15k-237	14,541	237	19.7±30	272,115	17,535	20,466
WN18RR	40,943	11	2.2±3.6	86,835	3,034	3,134
KINSHIP	104	25	82.2±3.5	8,544	1,068	1,074
UMLS	135	46	38.6±32.5	5,216	652	661

5.2. Training and optimization

We apply the same training strategy as [Dettmers et al. \(2018\)](#): Following the KvsAll training procedure,³ for a given pair (\mathbf{h}, \mathbf{r}) , we compute scores for all $x \in \mathcal{E}$ with $\phi(h, r, x)$ and apply the logistic sigmoid function $\sigma(\phi(h, r, x))$. Models are trained to minimize the binary cross entropy loss function, where $\hat{\mathbf{y}} \in \mathbb{R}^{|\mathcal{E}|}$ and $\mathbf{y} \in [0, 1]^{|\mathcal{E}|}$ denote the predicted scores and binary label vector, respectively.

$$L = -\frac{1}{|\mathcal{E}|} \sum_{i=1}^{|\mathcal{E}|} (\mathbf{y}^{(i)} \log(\hat{\mathbf{y}}^{(i)}) + (1 - \mathbf{y}^{(i)}) \log(1 - \hat{\mathbf{y}}^{(i)})). \quad (12)$$

We employ the Adam optimizer ([Kingma and Ba, 2014](#)), dropout ([Srivastava et al., 2014](#)), label smoothing and batch normalization ([Ioffe and Szegedy, 2015](#)) as similarly done in the literature ([Balažević et al., 2019b,c](#); [Dettmers et al., 2018](#); [Demir and Ngomo, 2021](#)). Moreover, we selected hyperparameters of our approaches by random search based on validation set performances ([Balažević et al., 2019c](#)). Notably, we did not search a good random seed for the random number generator and fixed the seed to 1 throughout our experiments.

5.3. Evaluation

We employ the standard metrics *filtered* Mean Reciprocal Rank (MRR) and hits at N (H@N) for link prediction ([Dettmers et al., 2018](#); [Balažević et al., 2019b](#)). For each test triple $(\mathbf{h}, \mathbf{r}, \mathbf{t})$, we construct its reciprocal $(\mathbf{t}, \mathbf{r}^{-1}, \mathbf{h})$ and add it into $\mathcal{G}^{\text{test}}$ which is a common technique to decrease the computational cost during testing ([Dettmers et al., 2018](#)). Then, for each test triple $(\mathbf{h}, \mathbf{r}, \mathbf{t})$, we compute the score of $(\mathbf{h}, \mathbf{r}, \mathbf{x})$ triples for all $x \in \mathcal{E}$ and calculate the filtered ranking $rank_t$ of the triple having t . Then we compute the MRR: $\frac{1}{|\mathcal{G}^{\text{test}}|} \sum_{(\mathbf{h}, \mathbf{r}, \mathbf{t}) \in \mathcal{G}^{\text{test}}} \frac{1}{rank_t}$. Consequently, given a $(\mathbf{h}, \mathbf{r}, \mathbf{t}) \in \mathcal{G}^{\text{test}}$, we compute ranks of missing entities based on *the rank of head and tail entities* as similarly done in [Balažević et al. \(2019b,c\)](#); [Dettmers et al. \(2018\)](#). For the sake of completeness, we also report link prediction performances based on *only tail rankings*, i.e., without including triples with reciprocal relations into test data, as similarly done by [Bansal et al. \(2019\)](#).

3. Here, we follow the terminology of [Ruffinelli et al. \(2019\)](#).

5.4. Implementation Details and Reproducibility

We implemented and evaluated our approach in the framework provided by [Balažević et al. \(2019c,a\)](#). To alleviate the hardware requirements for the reproducibility, we provide hyperparameter optimization, training and evaluation scripts along with pretrained models at the project page. Experiments were conducted on a single NVIDIA GeForce RTX 3090.

6. Results

Table 2 reports link prediction results on the WN18RR, FB15K-237 and YAGO3-10 datasets. Overall, the superior performance of our approaches becomes more and more apparent as the size and complexity of the knowledge graphs grows. On the smallest benchmark dataset (WN18RR), QMULT, OMULT, CONVQ and CONVO outperform many approaches including DistMult, ConvE and ComplEx in all metrics. However, QuatE, TuckER, and RotatE yield best performances. On the second-largest benchmark dataset (FB15K-237 is $3.1\times$ larger than WN18RR), CONVO outperforms all state-of-the-art approaches in 3 out of 4 metrics. Additionally, QMULT and CONVQ outperform all state-of-the-art approaches except for TuckER in terms of MRR, H@1 and H@3. On the largest benchmark dataset (YAGO3-10 is $12.4\times$ larger than WN18RR), QMULT, CONVO, CONVQ outperform all approaches in all metrics. Surprisingly, QMULT and OMULT reach the best and second-best performances in all metrics, whereas CONVO does not perform particularly well compared to our other approaches. CONVO outperforms QMULT, OMULT, and CONVQ in 8 out of 12 metrics, whereas QMULT yields better performance on YAGO3-10. Overall, these results suggest that superiority of learning hypercomplex embeddings becomes more apparent as the size and complexity of the input knowledge graph increases as measured by indegree (see Table 1) and PageRank (see Table 6 in [Dettmers et al. \(2018\)](#)). In Table 3, we compare some of best performing approaches on WN18RR, FB15K-237 and YAGO3-10 in terms of the number of trainable parameters. Results indicate that our approaches yield competitive performances (if not better) on all benchmark datasets.

6.1. Ensemble Learning

Table 4 reports link prediction results of ensembled models on benchmark datasets. Averaging the predicted scores of models improved the performances by circa 1–2% in MRR. These results suggest that performances may be further improved through optimizing the impact of each model in the ensemble.

6.2. Impact of Tail Entity Rankings

During our experiments, we observed that models often perform more accurately in predicting missing tail entities compared to predicting missing head entities which was also observed in [Bansal et al. \(2019\)](#). Table 5 indicates that MRR performances based on *only tail entity rankings* are on average absolute 10% higher than MRR results based on *head and tail entity rankings* on FB15K-237 while such difference was not observed on WN18RR.

Table 2: Link prediction results on WN18RR, F15K-237 and YAGO3-10. Results are obtained from corresponding papers. Bold and underlined entries denote best and second-best results. The dash(-) denotes values missing in the papers.

	WN18RR				FB15K-237				YAGO3-10			
	MRR	@1	@3	@10	MRR	@1	@3	@10	MRR	@1	@3	@10
TransE (Ruffinelli et al., 2019)	.228	.053	.368	.520	.313	.221	.347	.497	-	-	-	-
ConvE (Ruffinelli et al., 2019)	.442	.411	.451	.504	.339	.248	.359	.521	-	-	-	-
TuckER (Balažević et al., 2019c)	.470	.443	.482	.526	<u>.358</u>	<u>.266</u>	<u>.394</u>	.544	-	-	-	-
A2N (Bansal et al., 2019)	.450	.420	.460	.510	.317	.232	.348	.486	-	-	-	-
QuatE (Zhang et al., 2019)	.482	.436	.499	.572	.311	.221	.342	.495	-	-	-	-
HypER (Balažević et al., 2019b)	.465	.436	.477	.522	.341	.252	.376	.520	.533	.455	.580	.678
DistMult (Dettmers et al., 2018)	.430	.390	.440	.490	.240	.160	.260	.420	.340	.240	.380	.540
ConvE (Dettmers et al., 2018)	.430	.400	.440	.520	.335	.237	.356	.501	.440	.350	.490	.620
ComplEx (Dettmers et al., 2018)	.440	.410	.460	.510	.247	.158	.275	.428	.360	.260	.400	.550
REFE (Chami et al., 2020)	.455	.419	.470	.521	.302	.216	.330	.474	.370	.289	.403	.527
ROTE (Chami et al., 2020)	.463	.426	.477	.529	.307	.220	.337	.482	.381	.295	.417	.548
ATTE (Chami et al., 2020)	.456	.419	.471	.526	.311	.223	.339	.488	.374	.290	.410	.538
ComplEx-N3 (Chami et al., 2020)	.420	.390	.420	.460	.294	.211	.322	.463	.336	.259	.367	.484
MuRE (Chami et al., 2020)	.458	.421	.471	.525	.313	.226	.340	.489	.283	.187	.317	.478
RotatE (Sun et al., 2019)	<u>.476</u>	<u>.428</u>	<u>.492</u>	<u>.571</u>	.338	.241	.375	.533	.495	.402	.550	.670
QMULT	.438	.393	.449	.537	.346	.252	.383	.535	.555	.475	.602	.698
OMULT	.449	.406	.467	.539	.347	.253	.383	.534	<u>.543</u>	<u>.461</u>	<u>.592</u>	<u>.692</u>
CONVQ	.457	.424	.470	.525	.343	.251	.376	.528	.539	.459	.587	.687
CONVO	.458	.427	.473	.521	.366	.271	.403	<u>.543</u>	.489	.395	.546	.664

Table 3: Number of parameter comparisons on the WN18RR, F15K-237 and YAGO3-10 datasets. The dash(-) denotes values missing in the papers.

	WN18RR	FB15K-237	YAGO3-10
QuatE (Zhang et al., 2019)	16.38M	5.82M	-
RotatE (Sun et al., 2019)	40.95M	29.32M	123.22M
QMULT	16.38M	6.01M	49.30M
OMULT	16.38M	6.01M	49.30M
CONVQ	21.51M	11.13M	54.42M
CONVO	21.51M	11.13M	54.42M

Table 4: Link prediction results via ensembling models.

	WN18RR				FB15K-237				YAGO3-10			
	MRR	@1	@3	@10	MRR	@1	@3	@10	MRR	@1	@3	@10
Q-OMULT	.444	.399	.458	.544	.356	.260	.393	.545	<u>.557</u>	<u>.478</u>	.601	.700
QMULT-CONVQ	.446	.406	.455	.538	.357	.263	.392	.546	.561	.483	.606	.703
QMULT-CONVO	.449	.410	.459	.536	.372	.275	.411	.564	.543	.460	.594	.693
OMULT-CONVQ	.444	.403	.453	.537	.357	.262	.391	.547	.558	<u>.478</u>	<u>.602</u>	.700
OMULT-CONVO	.462	.425	.475	.539	.372	.277	.411	.564	.535	.450	.588	.692
CONVQ-O-OMULT	.463	.425	.475	.539	.372	<u>.275</u>	<u>.411</u>	<u>.567</u>	.552	.470	.599	<u>.702</u>

Table 5: Link prediction results based on only tail entity rankings.

	WN18RR				FB15K-237				YAGO3-10			
	MRR	@1	@3	@10	MRR	@1	@3	@10	MRR	@1	@3	@10
DistMult	.430	.410	.440	.480	.370	.275	.417	.568	-	-	-	-
ComplEx	.420	.380	.430	.480	.394	.303	.434	.572	-	-	-	-
ConvE	.440	.400	.450	.520	.410	.313	.457	.600	-	-	-	-
MINERVA	.450	.410	.460	.510	.293	.217	.329	.456	-	-	-	-
A2N	.490	.450	.500	.550	.422	.328	.464	.608	-	-	-	-
QMULT	.451	.403	.472	.553	.439	.341	.485	.636	.692	.626	.736	.799
OMULT	.461	.414	.482	<u>.559</u>	.440	.340	.486	.636	.689	.623	.733	.801
CONVQ	.470	.437	.482	.538	.441	.344	.482	.632	.674	.612	.715	.783
CONVO	.473	<u>.442</u>	<u>.491</u>	.535	.465	<u>.367</u>	.512	.654	.622	.535	.682	.774
Q-OMULT	.457	.401	.48	<u>.559</u>	.448	.347	.495	.644	<u>.696</u>	<u>.632</u>	.734	.804
QMULT-CONVQ	.466	.424	.480	.557	.451	.353	.496	.646	.697	.635	.737	<u>.803</u>
QMULT-CONVO	.474	.435	.487	.558	.467	.367	.516	.662	.680	.610	.727	.800
OMULT-CONVQ	.471	.430	.487	.560	.452	.354	.495	.647	<u>.696</u>	<u>.632</u>	.735	<u>.803</u>
OMULT-CONVO	.476	.436	.488	<u>.559</u>	<u>.466</u>	.366	<u>.515</u>	.662	.676	.602	.724	<u>.803</u>
CONVQ-O	<u>.477</u>	<u>.442</u>	<u>.494</u>	.548	.468	.370	.515	<u>.661</u>	.675	.603	.724	.795

Table 6: MRR link prediction results per relations on WN18RR. Ensemble refers to averaging predictions of CONVQ-CONVO-OMULT.

Relation Name	Rel. Type	RotatE	QMULT	CONVQ	OMULT	CONVO	Ensemble
hypernym	S	.15	.10	<u>.14</u>	.11	.13	.13
instance_hyponym	S	.32	.35	<u>.37</u>	.36	<u>.37</u>	.39
member_meronym	C	.23	<u>.22</u>	.20	.23	.20	.23
synset_domain_topic_of	C	.34	.31	.31	.32	<u>.33</u>	.34
has_part	C	<u>.18</u>	.19	.17	<u>.18</u>	<u>.18</u>	.19
member_of_domain_usage	C	<u>.32</u>	.29	.28	.27	.33	.29
member_of_domain_region	C	.20	.25	.38	.30	<u>.37</u>	.38
derivationally_related_form	R	.95	.98	.98	.98	.98	.98
also_see	R	.59	.67	.65	<u>.66</u>	<u>.66</u>	<u>.66</u>
verb_group	R	<u>.94</u>	1.0	1.0	1.0	1.0	1.0
similar_to	R	1.0	1.0	1.0	1.0	1.0	1.0

6.3. Link Prediction Per Relation and Direction

We reevaluate link prediction performances of some of the best-performing models from Table 2 in Tables 6 and 7. Allen et al. (2021) distinguish three types of relations: Type S relations are specialization relations such as `hypernym`, type C denote so-called generalized context-shifts and include `has_part` relations, and type R relations include so-called highly-related relations such as `similar_to`. Our results show that our approaches accurately rank missing tail and head entities for type R relations. For instance, our approaches perfectly rank (1.0 MRR) missing entities of symmetric relations (`verb_group` and `similar_to`). However, the direction of entity prediction has a significant impact on the results for non-symmetric type C relations. For instance, MRR performances of QMULT, CONVQ, OMULT and CONVO vary

Table 7: Link prediction results depending on the direction of prediction (head vs. tail prediction) on WN18RR. Ensemble refers to averaging predictions of CONVQ-CONVO-OMULT.

	QMULT	CONVQ	OMULT	CONVO	Ensemble
(h, r, x)					
hypernym	.12	.18	.13	.18	<u>.17</u>
instance_hyponym	.53	.56	.53	<u>.57</u>	.58
member_meronym	.17	.09	<u>.16</u>	.08	.14
synset_domain_topic_of	.49	.47	<u>.51</u>	.52	.52
has_part	.15	.12	.15	.14	.14
member_of_domain_usage	.04	.02	<u>.07</u>	.08	.05
member_of_domain_region	<u>.05</u>	.06	<u>.05</u>	.06	<u>.05</u>
derivationally_related_form	<u>.98</u>	<u>.98</u>	<u>.98</u>	<u>.98</u>	<u>.98</u>
also_see	.67	.63	<u>.65</u>	.63	.63
verb_group	1.0	1.0	1.0	1.0	1.0
similar_to	1.0	1.0	1.0	1.0	1.0
(x, r, t)					
hypernym	.07	<u>.09</u>	<u>.09</u>	.08	.10
instance_hyponym	.17	<u>.18</u>	.19	.17	.19
member_meronym	.27	.31	.29	.33	<u>.32</u>
synset_domain_topic_of	.13	<u>.14</u>	.13	.15	.15
has_part	<u>.22</u>	<u>.22</u>	<u>.22</u>	<u>.22</u>	.24
member_of_domain_usage	.53	<u>.54</u>	.47	.59	<u>.54</u>
member_of_domain_region	.45	<u>.69</u>	.55	.67	.70
derivationally_related_form	<u>.98</u>	<u>.98</u>	<u>.98</u>	.99	<u>.98</u>
also_see	<u>.68</u>	.67	.66	.69	<u>.68</u>
verb_group	1.0	1.0	1.0	1.0	1.0
similar_to	1.0	1.0	1.0	1.0	1.0

by up to absolute 0.63 for the relation `member_of_domain_region`. The low performances on `hypernym` (type S) may stem from the fact that there are 184 triples in the test split of WN18RR where `hypernym` occurs with entities of which at least one did not occur in the training split. Models often perform poorly on type C relations but considerably better on type R relations corroborating findings by [Allen et al. \(2021\)](#).

6.4. Batch vs. Unit Normalization

We investigate the effect of using batch-normalization instead of unit normalization as previously proposed by [Zhang et al. \(2019\)](#). Table 8 indicates that the scaling effect of hypercomplex multiplications can be effectively alleviated by using the batch normalization technique. Replacing unit normalization with the batch normalization technique allows benefiting (1) from its regularization effect and (2) from its numerical stability. Through batch normalization, our models are able to control the rate of normalization and benefit from its implicit regularization effect ([Ioffe and Szegedy, 2015](#)).

6.5. Convergence on YAGO3-10

Figure 1 indicates that incurred binary cross entropy losses significantly decrease within the first 100 epochs. After the 300th iteration, CONVQ and CONVO appear to converge as losses do not fluctuate, whereas training losses of QMULT and OMULT continue fluctuating.

Table 8: Batch normalization vs. unit normalization for link prediction.

	Kinship				UMLS			
	MRR	H@1	@3	@10	MRR	@1	@3	@10
GNTP-Standard Minervini et al. (2019)	.72	.59	.82	.96	.80	.70	.88	.95
GNTP-Attention Minervini et al. (2019)	.76	.64	.85	.96	.86	.76	.95	.98
NTP Minervini et al. (2019)	.35	.24	.37	.57	.80	.70	.88	.95
NeuralLP Minervini et al. (2019)	.62	.48	.71	.91	.78	.64	.87	.96
MINERVA Minervini et al. (2019)	.72	.60	.81	.92	.83	.73	.90	.97
ConvE Dettmers et al. (2018)	.83	.74	.92	<u>.98</u>	.94	.92	.96	<u>.99</u>
QMULT (batch)	.88	.81	.94	.99	<u>.96</u>	.93	.98	1.0
QMULT (unit)	.69	.58	.78	.90	.77	.69	.82	.93
CONVQ (batch)	.86	.77	.93	<u>.98</u>	.92	.86	.98	1.0
CONVQ (unit)	.61	.49	.68	.85	.55	.45	.59	.75
OMULT (batch)	.87	.80	.94	.99	.95	.91	.98	1.0
OMULT (unit)	.69	.57	.77	.89	.76	.66	.82	.93
CONVO (batch)	.86	.77	.93	<u>.98</u>	.90	.82	.98	1.0
CONVO (unit)	.65	.53	.72	.86	.56	.46	.61	.78

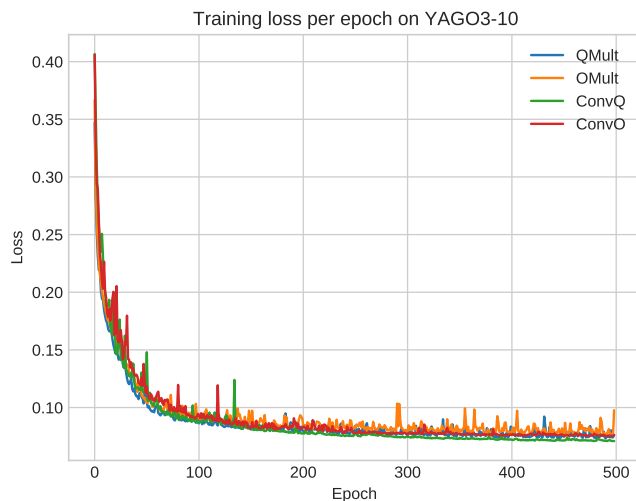


Figure 1: Convergence on the training set.

6.6. Link Prediction Results on Previous Benchmark Datasets

Table 9 reports results on WN18 and FB15K showing that our approaches CONVQ and CONVO outperform state-of-the-art approaches in 6 out of 8 metrics on the datasets.

7. Discussion

Our approaches often outperform many state-of-the-art approaches on all datasets. QMULT and OMULT outperform many state-of-the-art approaches including DistMult and ComplEx. These results indicate that scoring functions based on hypercomplex multiplications are more

Table 9: Link prediction results on WN18 and FB15K.

Model	WN18					FB15K				
	Param.	MRR	Hit@10	Hit@3	Hit@1	Param.	MRR	Hit@10	Hit@3	Hit@1
TransE	-	.495	.943	.888	.113	-	.463	.749	.578	.297
TransR	-	.605	.940	.876	.335	-	.346	.582	.404	.218
ER-MLP	-	.712	.863	.775	.626	-	.288	.501	.317	.173
RESCAL	-	.890	.928	.904	.842	-	.354	.587	.409	.235
HolE	-	.938	.949	.945	.930	-	.524	.739	.613	.402
Simple	-	.942	.947	.944	.939	-	.727	.838	.773	.660
TorusE	-	.947	.954	.950	.943	-	.733	.832	.771	.674
RotatE	-	.947	.961	.953	.938	-	.699	.872	.788	.585
QuatE	-	.949	.960	.954	.941	-	.770	.878	.821	.700
QuatE ²	-	.950	.962	.954	.944	-	.833	.900	.859	.800
QMULT	16.39M	<u>.975</u>	<u>.980</u>	<u>.976</u>	<u>.972</u>	7.05M	.755	<u>.896</u>	.819	.668
OMULT	16.39M	<u>.975</u>	.981	<u>.976</u>	<u>.972</u>	7.05M	.748	.889	.813	.660
CONVQ	21.51M	.976	<u>.980</u>	.977	.973	12.17M	<u>.813</u>	.923	.868	<u>.743</u>
CONVO	21.51M	.976	<u>.980</u>	.977	.973	12.17M	.810	.923	<u>.865</u>	.739

effective than scoring functions based on real and complex multiplications. This observation corroborates findings of Zhang et al. (2019). CONVO often perform slightly better than CONVQ on all datasets. Additionally, QMULT and OMULT perform particularly well on YAGO3-10. These results may stem from the fact that CONVQ and CONVO may benefit from initializing parameters with the correct variance as highlighted in Hanin and Rolnick (2018). Overall, superior performances of our models stem from (1) hypercomplex embeddings and (2) the inclusion of convolution operations. Our models are allowed to degrade into ComplEx or DistMult if necessary (see Section 4). Inclusion of the convolution operation followed by an affine transformation permits to find a good ratio between expressiveness and the number of parameters.

8. Conclusion

In this study, we presented effective compositions of convolution operations with hypercomplex multiplications in the quaternion and octonion algebras to address the link prediction problem. Experimental results showed that QMULT and OMULT performing hypercomplex multiplication on hypercomplex-valued embeddings of entities and relations are effective methods to tackle the link prediction problem. CONVQ and CONVO forge QMULT and OMULT with convolution operations followed by an affine transformation. By virtue of this novel composition, CONVQ and CONVO facilitate to find a good ratio between expressiveness and the number of parameters. Experiments suggest that (1) generalizing real- and complex-valued models such as DistMult and ComplEx to the hypercomplex space is beneficial, particularly for larger knowledge graphs, (2) the scaling effect of hypercomplex multiplication can be more effectively tackled with batch normalization than unit normalization, and (3) the application of ensembling can be used to further increase generalization performances.

In future work, we plan to investigate the generalization of our approaches to temporal knowledge graphs and translation based models on hypercomplex vector spaces.

References

- Carl Allen, Ivana Balazevic, and Timothy Hospedales. Interpreting knowledge graph relation representation from word embeddings. In *International Conference on Learning Representations*, 2021.
- John Baez. The octonions. *Bulletin of the American Mathematical Society*, 39(2):145–205, 2002.
- Ivana Balažević, Carl Allen, and Timothy Hospedales. Multi-relational poincaré graph embeddings. In *Advances in Neural Information Processing Systems*, pages 4465–4475, 2019a.
- Ivana Balažević, Carl Allen, and Timothy M Hospedales. Hypernetwork knowledge graph embeddings. In *International Conference on Artificial Neural Networks*, pages 553–565. Springer, 2019b.
- Ivana Balažević, Carl Allen, and Timothy M Hospedales. Tucker: Tensor factorization for knowledge graph completion. *arXiv preprint arXiv:1901.09590*, 2019c.
- Trapit Bansal, Da-Cheng Juan, Sujith Ravi, and Andrew McCallum. A2n: attending to neighbors for knowledge graph inference. In *Proceedings of the 57th Annual Meeting of the Association for Computational Linguistics*, pages 4387–4392, 2019.
- Antoine Bordes, Sumit Chopra, and Jason Weston. Question answering with subgraph embeddings. *arXiv preprint arXiv:1406.3676*, 2014.
- Hongyun Cai, Vincent W Zheng, and Kevin Chen-Chuan Chang. A comprehensive survey of graph embedding: Problems, techniques, and applications. *IEEE Transactions on Knowledge and Data Engineering*, 30(9):1616–1637, 2018.
- Ines Chami, Adva Wolf, Da-Cheng Juan, Frederic Sala, Sujith Ravi, and Christopher Ré. Low-dimensional hyperbolic knowledge graph embeddings. *arXiv preprint arXiv:2005.00545*, 2020.
- Heng Chen, Weimei Wang, Guanyu Li, and Yimin Shi. A quaternion-embedded capsule network model for knowledge graph completion. *IEEE Access*, 2020.
- Caglar Demir and Axel-Cyrille Ngonga Ngomo. Convolutional complex knowledge graph embeddings. In *Eighteenth Extended Semantic Web Conference - Research Track*, 2021.
- Tim Dettmers, Pasquale Minervini, Pontus Stenetorp, and Sebastian Riedel. Convolutional 2d knowledge graph embeddings. In *Thirty-Second AAAI Conference on Artificial Intelligence*, 2018.
- Jeffrey Scott Eder. Knowledge graph based search system, June 21 2012. US Patent App. 13/404,109.
- Ian Goodfellow, Yoshua Bengio, and Aaron Courville. *Deep learning*. MIT press, 2016.

- William Rowan Hamilton. Lxxviii. on quaternions; or on a new system of imaginaries in algebra: To the editors of the philosophical magazine and journal. *The London, Edinburgh, and Dublin Philosophical Magazine and Journal of Science*, 25(169):489–495, 1844.
- Boris Hanin and David Rolnick. How to start training: The effect of initialization and architecture. *arXiv preprint arXiv:1803.01719*, 2018.
- Kaiming He, Xiangyu Zhang, Shaoqing Ren, and Jian Sun. Deep residual learning for image recognition. In *Proceedings of the IEEE conference on computer vision and pattern recognition*, pages 770–778, 2016.
- Aidan Hogan, Eva Blomqvist, Michael Cochez, Claudia d’Amato, Gerard de Melo, Claudio Gutierrez, José Emilio Labra Gayo, Sabrina Kirrane, Sebastian Neumaier, Axel Polleres, et al. Knowledge graphs. *arXiv preprint arXiv:2003.02320*, 2020.
- Sergey Ioffe and Christian Szegedy. Batch normalization: Accelerating deep network training by reducing internal covariate shift. *arXiv preprint arXiv:1502.03167*, 2015.
- Shaoxiong Ji, Shirui Pan, Erik Cambria, Pekka Marttinen, and Philip S Yu. A survey on knowledge graphs: Representation, acquisition and applications. *arXiv preprint arXiv:2002.00388*, 2020.
- Diederik P Kingma and Jimmy Ba. Adam: A method for stochastic optimization. *arXiv preprint arXiv:1412.6980*, 2014.
- Timothée Lacroix, Nicolas Usunier, and Guillaume Obozinski. Canonical tensor decomposition for knowledge base completion. *arXiv preprint arXiv:1806.07297*, 2018.
- Haonan Lu and Hailin Hu. Dense: An enhanced non-abelian group representation for knowledge graph embedding. *arXiv preprint arXiv:2008.04548*, 2020.
- Stanislav Malyshev, Markus Krötzsch, Larry González, Julius Gonsior, and Adrian Bielefeldt. Getting the most out of wikidata: semantic technology usage in wikipedia’s knowledge graph. In *International Semantic Web Conference*, pages 376–394. Springer, 2018.
- Pasquale Minervini, Matko Bošnjak, Tim Rocktäschel, Sebastian Riedel, and Edward Grefenstette. Differentiable reasoning on large knowledge bases and natural language. *arXiv preprint arXiv:1912.10824*, 2019.
- Diego Moussallem, Axel-Cyrille Ngonga Ngomo, Paul Buitelaar, and Mihael Arcan. Utilizing knowledge graphs for neural machine translation augmentation. In *Proceedings of the 10th International Conference on Knowledge Capture, K-CAP ’19*, pages 139–146, New York, NY, USA, 2019. ACM. ISBN 978-1-4503-7008-0.
- Dai Quoc Nguyen, Tu Dinh Nguyen, Dat Quoc Nguyen, and Dinh Phung. A novel embedding model for knowledge base completion based on convolutional neural network. *arXiv preprint arXiv:1712.02121*, 2017.
- Maximilian Nickel, Volker Tresp, and Hans-Peter Kriegel. A three-way model for collective learning on multi-relational data. In *ICML*, volume 11, pages 809–816, 2011.

- Maximilian Nickel, Kevin Murphy, Volker Tresp, and Evgeniy Gabrilovich. A review of relational machine learning for knowledge graphs. *Proceedings of the IEEE*, 104(1):11–33, 2015.
- Titouan Parcollet, Ying Zhang, Mohamed Morchid, Chiheb Trabelsi, Georges Linarès, Renato De Mori, and Yoshua Bengio. Quaternion convolutional neural networks for end-to-end automatic speech recognition. *arXiv preprint arXiv:1806.07789*, 2018.
- Titouan Parcollet, Mirco Ravanelli, Mohamed Morchid, Georges Linarès, Chiheb Trabelsi, Renato De Mori, and Yoshua Bengio. Quaternion recurrent neural networks, 2019.
- Daniel Ruffinelli, Samuel Broscheit, and Rainer Gemulla. You can teach an old dog new tricks! on training knowledge graph embeddings. In *International Conference on Learning Representations*, 2019.
- Muhammad Saleem, Maulik R Kamdar, Aftab Iqbal, Shanmukha Sampath, Helena F Deus, and Axel-Cyrille Ngonga Ngomo. Big linked cancer data: Integrating linked tcga and pubmed. *Journal of web semantics*, 27:34–41, 2014.
- Nitish Srivastava, Geoffrey Hinton, Alex Krizhevsky, Ilya Sutskever, and Ruslan Salakhutdinov. Dropout: a simple way to prevent neural networks from overfitting. *The journal of machine learning research*, 15(1):1929–1958, 2014.
- Zhiqing Sun, Zhi-Hong Deng, Jian-Yun Nie, and Jian Tang. Rotate: Knowledge graph embedding by relational rotation in complex space. *arXiv preprint arXiv:1902.10197*, 2019.
- Théo Trouillon, Johannes Welbl, Sebastian Riedel, Éric Gaussier, and Guillaume Bouchard. Complex embeddings for simple link prediction. In *ICML*, pages 2071–2080, 2016.
- Théo Trouillon, Christopher R Dance, Éric Gaussier, Johannes Welbl, Sebastian Riedel, and Guillaume Bouchard. Knowledge graph completion via complex tensor factorization. *The Journal of Machine Learning Research*, 18(1):4735–4772, 2017.
- Bishan Yang, Wen-tau Yih, Xiaodong He, Jianfeng Gao, and Li Deng. Embedding entities and relations for learning and inference in knowledge bases. In *ICLR*, 2015.
- Aston Zhang, Yi Tay, Shuai Zhang, Alvin Chan, Anh Tuan Luu, Siu Cheung Hui, and Jie Fu. Beyond fully-connected layers with quaternions: Parameterization of hypercomplex multiplications with $1/n$ parameters. *arXiv preprint arXiv:2102.08597*, 2021.
- Fuzheng Zhang, Nicholas Jing Yuan, Defu Lian, Xing Xie, and Wei-Ying Ma. Collaborative knowledge base embedding for recommender systems. In *KDD*, pages 353–362. ACM, 2016.
- Shuai Zhang, Yi Tay, Lina Yao, and Qi Liu. Quaternion knowledge graph embeddings. In *Advances in Neural Information Processing Systems*, pages 2731–2741, 2019.